RHEUMATOLOGY

Rheumatology 2023;62:1306–1316
https://doi.org/10.1093/rheumatology/keac411
Advance access publication 28 July 2022

Original article

Reduced Cathepsin L expression and secretion into the extracellular milieu contribute to lung fibrosis in systemic sclerosis

Joe E. Mouawad[1,2], Shailza Sharma[1], Ludivine Renaud[1], Joseph M. Pilewski[3], Satish N. Nadig[4] and Carol Feghali-Bostwick[1]

Abstract

Objectives. Lung fibrosis is the leading cause of death in SSc, with no cure currently available. Antifibrotic Endostatin (ES) production does not reach therapeutic levels in SSc patients, suggesting a deficit in its release from Collagen XVIII by the main cleavage enzyme, Cathepsin L (CTSL). Thus, elucidating a potential deficit in CTSL expression and activity unravels an underlying molecular cause for SSc-driven lung fibrosis.

Methods. Fibrosis was induced experimentally using TGF-β *in vitro*, in primary human lung fibroblasts (pLFs), and *ex vivo*, in human lung tissues. ES and CTSL expression was quantified using ELISA, RT-qPCR, immunoblotting or immunofluorescence. Recombinant NC1-FLAG peptide was used to assess CTSL cleavage activity. CTSL expression was also compared between SSc *vs* normal (NL)-derived pLFs and lung tissues.

Results. ES levels were significantly reduced in media conditioned by TGF-β-induced pLFs. TGF-β-stimulated pLFs significantly reduced expression and secretion of CTSL into the extracellular matrix (ECM). CTSL was also sequestered in its inactive form into extracellular vesicles, further reducing its availability in the ECM. Media conditioned by TGF-β-induced pLFs showed reduced cleavage of NC1-Flag and reduced release of the antifibrotic ES fragment. SSc-derived pLFs and lung tissues expressed significantly lower levels of CTSL compared with NL.

Conclusions. Our findings identify CTSL as a protein protective against lung fibrosis via its activation of antifibrotic ES, and whose expression in SSc pLFs and lung tissues is suppressed. Identifying strategies to boost CTSL endogenous levels in SSc patients could serve as a viable therapeutic strategy.

Key words: SSc, scleroderma, lung, fibrosis, fibroblasts, extracellular vesicles, TGF-β, Cathepsin L, endostatin

BASIC SCIENCE

Rheumatology key messages

- Cathepsin L (CTSL) exerts anti-fibrotic effects by cleaving Collagen XVIII to release endostatin.
- CTSL expression and secretion into the extracellular milieu of lung fibroblasts is reduced upon TGF-β activation.
- SSc lung fibroblasts and tissues express significantly lower levels of CTSL compared with normal controls.

Introduction

Fibrosis is characterized by the excessive accumulation of connective tissue components which form the extracellular matrix (ECM) [1]. Progressive fibrosis is a major cause of morbidity and mortality in individuals suffering from SSc, which is one of the most lethal rheumatic diseases [2]. Pulmonary fibrosis stands as the leading cause of death in SSc [3]. Currently, there is no cure for SSc, and treatment is limited to symptomatic alleviation addressing the comorbidities but not the fibrosis of the skin and various visceral organs. Two recently Food and Drug Administration–approved drugs for SSc merely reduce the progression of interstitial lung disease [4, 5]. Thus, there is a need to investigate novel molecular pathways involved in fibrosis,

[1]Division of Rheumatology & Immunology, Department of Medicine, [2]Medical Scientist Training Program, Medical University of South Carolina, Charleston, SC, [3]Division of Pulmonary, Allergy & Critical Care Medicine, Department of Medicine, University of Pittsburgh School of Medicine, Pittsburgh, PA and [4]Division of Organ Transplantation, Department of Surgery, Northwestern University Feinberg School of Medicine, Chicago, IL, USA

Submitted 2 May 2022; accepted 8 July 2022

Correspondence to: Carol Feghali-Bostwick, Division of Rheumatology & Immunology, Department of Medicine, Medical University of South Carolina, 96 Jonathan Lucas St, MSC 637, Charleston, SC 29425 USA.
E-mail: feghalib@musc.edu

© The Author(s) 2022. Published by Oxford University Press on behalf of the British Society for Rheumatology. All rights reserved. For permissions, please email: journals.permissions@oup.com

especially lung fibrosis in the context of SSc, to find potential therapeutic treatments.

Endostatin (ES), widely known for its antiangiogenic activity, is a natural proteolytic fragment from the C-terminus of Collagen XVIII, a proteoglycan located in basement membranes and walls of blood vessels [6]. We showed that ES has potent anti-fibrotic activity [7–9]. The discovery of this novel function of ES poses an interesting question as to how ES release is regulated during fibrosis in SSc. This is especially important since ES levels are detected in lung lavage fluid and the circulation of patients with lung fibrosis [10, 11]; however, those levels do not reach anti-fibrotic concentrations [8], suggesting that the natural anti-fibrotic response is blunted in the setting of fibrosis.

The major catalytic enzyme known to cleave and activate ES from Collagen XVIII is Cathepsin L (CTSL), a lysosomal cysteine peptidase that can be secreted by cells [12, 13]. Recent studies have shown that fibrosis is associated with lower CTSL expression levels in the affected areas, especially with dermal fibrosis in SSc patients [14, 15], suggesting CTSL may have antifibrotic properties. Apart from secretion into the ECM, CTSL can also localize into extracellular vesicles (EVs) [16, 17]. EVs are membrane-bound vesicles released by all cells, serving as an intercellular communication tool via transfer of nucleic acids and proteins [18]. Recently, the role of EVs in lung physiology and pathology has been highlighted [19], shedding light on a new mechanism in the context of lung fibrosis. Taken together, we hypothesized that a decrease in CTSL availability in the extracellular milieu, via decreased secretion or possibly via sequestration in EVs, would blunt the release of antifibrotic ES, promoting the spread of fibrosis.

TGF-β has long been shown to be a master promoter of fibrosis [20]. It is a potent inducer of fibroblast differentiation into myofibroblasts, which are the effector cells in the initiation and development of fibrosis via ECM deposition [20, 21]. Investigating TGF-β-regulated genes in fibrotic lungs and skin of SSc patients has shown that increased expression of these genes correlates with disease activity, highlighting the role of TGF-β as a central mediator of pathogenesis in SSc [22]. As such, we questioned whether CTSL expression, and hence ES activation, could be suppressed by TGF-β signalling and serve as one of the driving forces for lung fibrosis in SSc patients. We therefore evaluated CTSL expression and activity under fibrotic conditions via the TGF-β experimental model of fibrosis *in vitro*, using primary human lung fibroblasts (pLFs), and *ex vivo*, using lung tissues in organ culture. We also assessed the possibility of CTSL sequestration in EVs of pLFs. Finally, we compared CTSL expression in SSc-derived pLFs and lung tissues to those derived from healthy lungs.

Methods

Lung tissues

Lung tissues were obtained from organ donors (normal lung; NL) whose lungs were not used for transplantation, under a protocol approved by the Institutional Review Board of the Medical University of South Carolina. Lung tissues were also obtained from patients with SSc undergoing lung transplantation at the University of Pittsburgh Medical center under a protocol approved by the Institutional Review Board of the University of Pittsburgh and following written consent. All SSc patients had pulmonary fibrosis with no evidence of secondary pulmonary hypertension.

Primary human lung fibroblast culture

Human primary lung fibroblasts (pLFs) were cultured from lung tissues of SSc patients undergoing lung transplantation following written consent as previously described [23]. Primary fibroblasts were also cultured from the lung tissues of normal donors whose lungs were not used for transplantation [24]. Briefly, ~2–3 mm^2 pieces of tissue were minced and fibroblasts were cultured and maintained in DMEM (10-013-CM, Corning, Corning, NY, USA) supplemented with 10% fetal bovine serum (F4135, Sigma-Aldrich, St Louis, MO, USA), penicillin, streptomycin, and antimycotic agent (A5955, Sigma-Aldrich, St Louis, MO, USA). Fibroblasts were used in passages 3–8.

In vitro fibroblast stimulation

Actively growing pLFs were stimulated as previously described with some modifications [9]. Briefly, 2.0×10^5 pLFs were plated in 6-well tissue culture plates in 10% fetal bovine serum–containing DMEM. At 70–80% confluence, the cells were starved in serum-free DMEM media (SFM) for 1 h prior to stimulation with 5 ng/ml recombinant TGF-β1 (240-B, R&D Systems, Minneapolis, MN, USA) or the same volume of vehicle (4 mM HCl + 0.1% BSA) and harvested after 24, 48, 72 and 96 h for RNA and protein extraction. Conditioned media were also collected at each timepoint to analyse secreted proteins. Samples were stored at −80°C.

Ex vivo human lung culture and stimulation

Human lung tissues in organ culture were prepared as previously described [9, 25]. Briefly, normal human lung tissues were sliced and 5 mm^2 cores were obtained. Two cores were placed in each well of a 6-well plate in serum-free DMEM supplemented with penicillin, streptomycin and antimycotic agent. Lung tissue cores were treated with 10 ng/ml recombinant TGF-β1; 4 mM HCl + 0.1% BSA was used as vehicle control. RNA and protein were extracted from lung tissues after 24, 48, 72 and 96 h of incubation. Lung tissues at 96 h were also fixed in 10% formalin and embedded in paraffin for sectioning and immunofluorescence.

RNA sequencing and differential expression analysis

RNA sequencing was done at Novogene Corporation Inc. (Sacramento, CA, USA) as we previously described [26]. The heatmap was generated from the normalized counts for genes of interest using MORPHEUS software (https://software.broadinstitute.org/morpheus/).

Statistical analysis

All continuous variables were expressed as the mean (S.E.M.). Statistical comparisons between two groups were performed using 2-tailed Student's *t*-test, and between three or more groups using analysis of variance, as specified in figure legends. GraphPad Prism 9 was used for all statistical analyses. *P*-values <0.05 were considered statistically significant.

Please see additional methods in the supplementary material, available at *Rheumatology* online.

Results

TGF-β induction reduces ES protein levels released by pLFs

To examine the effect of TGF-β on ES protein levels, we stimulated pLFs from control donors with TGF-β. ES protein levels were significantly reduced in media conditioned by activated fibroblasts, showing 28% ($P = 0.0621$) and 33% ($P < 0.01$) reduction at 48 h and 72 h, respectively (Fig. 1A). We then evaluated the transcription levels of the parent molecule, Collagen XVIII (*COL18A1*). Fibrotic induction in pLFs had no significant effect on *COL18A1* transcription at 24 h and 48 h but increased it 27% ($P < 0.05$) at 72 h (Fig. 1B). These findings suggest that the reduction in ES protein levels following TGF-β stimulation is not due to decreased transcription of the corresponding gene.

CTSL expression and secretion are downregulated in TGF-β-induced pLFs

CTSL is the major cysteine peptidase responsible for cleavage and release of ES from Collagen XVIII [12, 13]. We thus evaluated the effect of TGF-β on CTSL expression in pLFs. CTSL mRNA levels were significantly downregulated in TGF-β-activated pLFs, with 21% reduction at 24 h ($P = 0.0552$), 62% at 48 h ($P < 0.0001$), and 53% at 72 h ($P < 0.0001$) (Fig. 1C). The reduction was also observed at the protein level both in lysates and conditioned media, with 47% reduction at 48 h ($P = 0.0602$) and 56% at 72 h ($P < 0.05$) in lysates (Fig. 1D).

Fig. 1 Activated pLFs release reduced levels of ES and downregulate CTSL expression and secretion

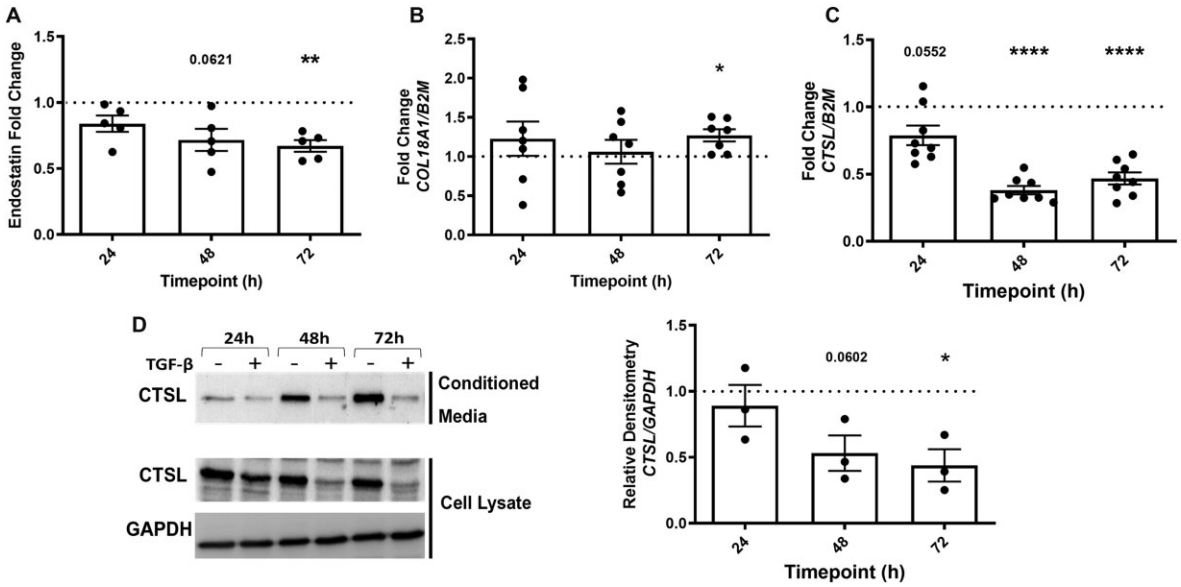

pLFs from different donors were treated with vehicle control (VC) or 5 ng/ml recombinant TGF-β. Supernatants and RNA were collected after 24, 48 and 72 h of stimulation. (**A**) ES concentrations in the supernatants were measured using ELISA, and fold-change estimates were calculated to compare TGF-β with vehicle ($n = 5$, three donors). (**B**) *COL18A1* gene expression levels were quantified using qPCR, and fold-change estimates were calculated to compare TGF-β to vehicle (normalized to *B2M*) ($n = 7$, four donors). (**C**) *CTSL* gene expression levels were quantified using qPCR, and fold-change estimates were calculated to compare TGF-β to vehicle (normalized to *B2M*) ($n = 8$, four donors). (**D**) CTSL was detected in conditioned media and cellular lysates. GAPDH was used as a loading control for cellular lysates to which the band density quantification was normalized. ($n = 3$, three donors). Graphs analysed by 1-way analysis of variance (Dunnett correction). A dotted line at a fold-change of 1.0 (i.e. no change) is provided for reference. Bars represent mean (S.E.M.). *$P < 0.05$, **$P < 0.01$, ****$P < 0.0001$. pLF: primary human lung fibroblast; ES: Endostatin; CTSL: Cathepsin L; COL18A1: collagen type XVIII alpha 1 chain; B2M: β2-microglobulin; GAPDH: glyceraldehyde-3-phosphate dehydrogenase.

CTSL expression in pLFs is inhibited by the TGF-β canonical pathway

TGF-β can signal via canonical and non-canonical pathways [20]. Inhibiting the canonical TGF-β pathway in pLFs, using a selective Smad3 inhibitor (SIS3) [27], abrogated the TGF-β-induced fibrosis, as indicated by the inhibition of mRNA and protein expression and secretion of the ECM component COL1α1 (supplementary Figs S1A and B, available at *Rheumatology* online). The opposite effect was seen on CTSL expression, which showed a reversal of the TGF-β-induced inhibition upon SIS3 treatment, at both the RNA and protein levels ($P < 0.05$) (Fig. 2A and B). Interestingly, SIS3 alone induced a significant increase in CTSL expression ($P < 0.05$), suggesting that the Smad pathway downstream of TGF-β suppresses CTSL expression constitutively in pLFs. In contrast, inhibiting the major noncanonical pathways of TGF-β, including the PI3K, JNK and MEK pathways [20], did not rescue the reduction of CTSL expression, but further reduced it, albeit insignificantly (supplementary Fig. S2A and B, available at *Rheumatology* online). These data demonstrate that TGF-β-induced reduction of CTSL in pLFs occurs via the canonical Smad-mediated pathway.

Reduction of ES release is mediated via the downregulation of CTSL upon TGF-β induction

To determine whether the reduction in ES release upon TGF-β treatment is caused by the decrease in CTSL levels, we designed a recombinant C-terminal Flag-tagged NC1 peptide (NC1-Flag), which corresponds to the NC1 domain of Collagen XVIII, encompassing the ES peptide and upstream CTSL cleavage site [12]. The expression was confirmed by immunoblotting (Fig. 3A). Using the purified recombinant peptide, we assessed ES cleavage activity in pLF-conditioned SFM by quantifying the cleavage levels of NC1-Flag via immunoblotting. We found that SFM from TGF-β-treated pLFs had significantly reduced NC1-Flag cleavage activity when compared with vehicle-treated pLFs. NC1-Flag was cleaved rapidly over 24 h in the SFM conditioned by vehicle-treated pLFs, achieving significant reduction in levels at 6 h ($P < 0.05$) and 24 h ($P < 0.01$) when compared with 1 h. NC1-Flag remained mostly intact in the SFM conditioned by TGF-β-treated pLFs, showing a reduction only at 24 h that was significant yet more modest than the vehicle group ($P < 0.05$) (Fig. 3B). To show that this outcome is specific to the TGF-β-induced reduction in CTSL levels, we treated media from vehicle-treated pLFs with a selective CTSL inhibitor (CTSLi). CTSL inhibition

Fig. 2 CTSL expression in pLF is specifically inhibited by TGF-β's canonical pathway

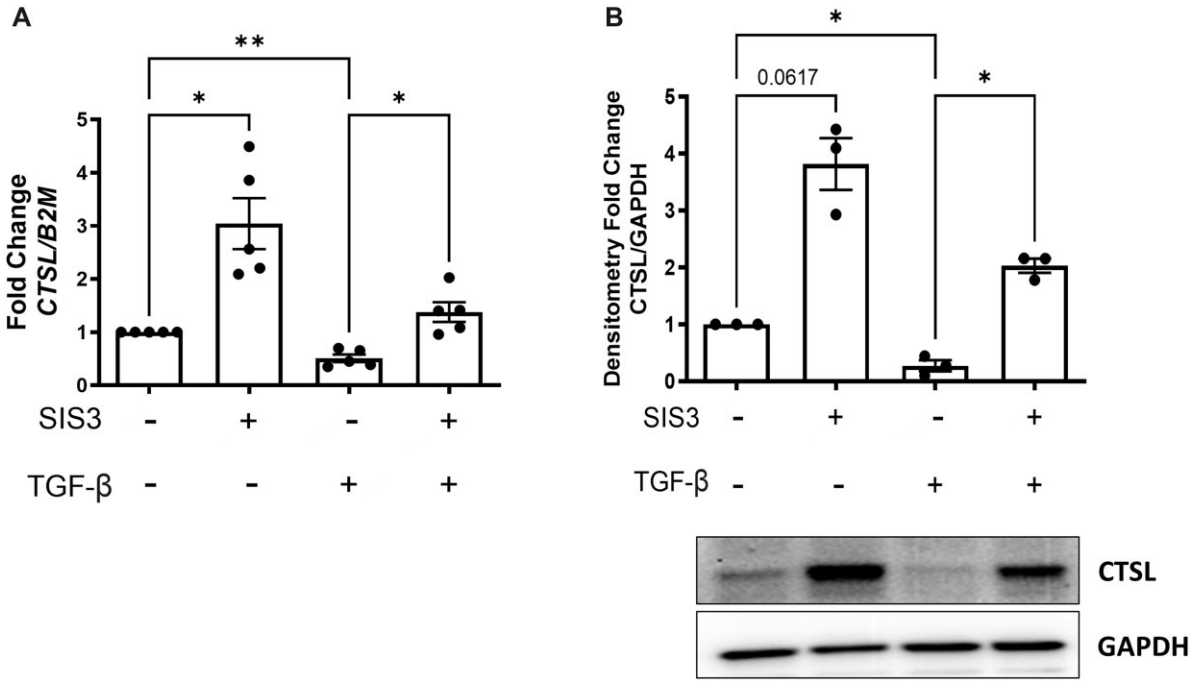

NL fibroblasts from different donors were treated with vehicle control, recombinant TGF-β and/or SIS3 (4 μM), PI3K inhibitor (10 μM), or JNK inhibitor (10 μM). Lysates and RNA were collected after 48 h. (**A**) Gene expression levels of *CTSL* were quantified using qPCR ($n = 5$, three donors), and fold-change estimates were calculated to compare treated samples with the untreated one (normalized to B2M). (**B**) Protein expression levels of CTSL were analysed by immunoblotting, with GAPDH used as loading control ($n = 3$, three donors). Graphs analysed by 1-Way analysis of variance (Dunnett correction). Bars represent mean (S.E.M.). *$P < 0.05$, **$P < 0.01$. pLF: primary human lung fibroblast; NL: normal lung; SIS3: smad3 inhibitor; CTSL: Cathepsin L; GAPDH: glyceraldehyde-3-phosphate dehydrogenase.

FIG. 3 TGF-β reduces cleavage of NC1-Flag via downregulation of CTSL

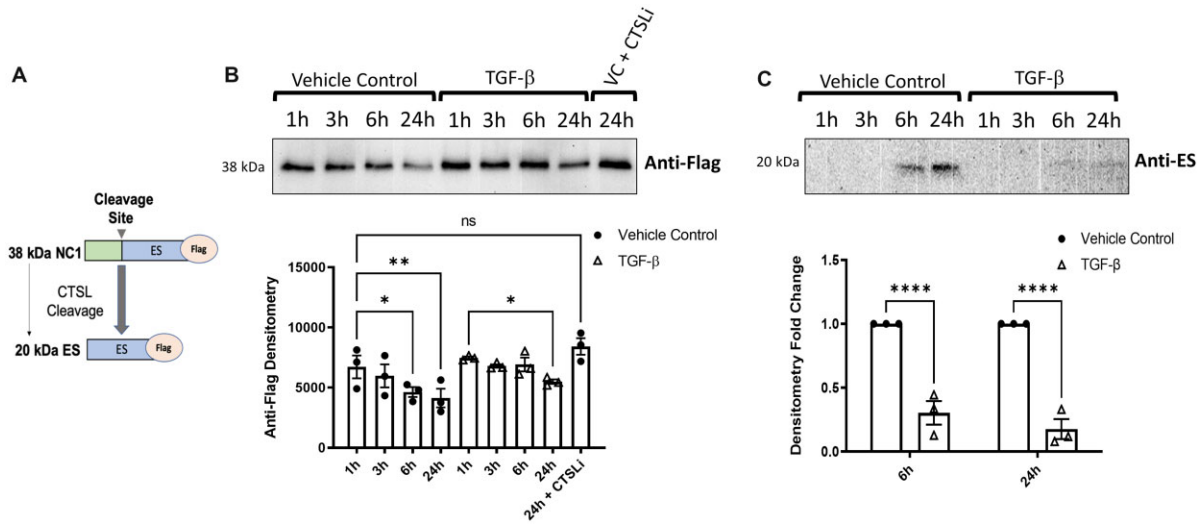

(**A**) Expression of recombinant flag-tagged NC1 peptide. NC1 coding sequence was inserted in a flag tag overexpression plasmid and transfected into HEK 293 cells for 96 h. Empty plasmid transfection was used as control. (**B**) NL fibroblasts from different donors were treated with vehicle control or recombinant TGF-β. Supernatants were collected after 72 h of stimulation, inoculated with recombinant NC1-Flag, and incubated for 1, 3, 6 and 24 h at 37°C. A selective CTSL inhibitor (CTSLi, 20 μM) was used in parallel on a VC-treated sample for 24 h. Cleavage of NC1-Flag was detected via immunoblotting. (**C**) Generated ES was detected via immunoblotting at 6 and 24 h, using ES specific antibody ($n = 3$, three donors). Graphs analysed by (B) 1-way analysis of variance (Dunnett correction) and (C) 2-way analysis of variance (Šídák correction). Bars represent mean (S.E.M.). $^{*}P < 0.05$, $^{**}P < 0.01$, $^{****}P < 0.0001$, ns: not significant. CTSL: Cathepsin L; ES: endostatin; VC: vehicle control.

abrogated the cleavage of the NC1-Flag peptide over 24 h (Fig. 3B). Consequently, the cleaved ES product appeared after 6 h and 24 h of incubation in the vehicle-treated SFM, at levels significantly greater than those detected in TGF-β-treated pLF SFM ($P < 0.0001$ at both 6 and 24 h) (Fig. 3C and supplementary Fig. S3, available at *Rheumatology* online). These findings demonstrate that the reduced cleavage of ES from the NC1 domain is mediated by the TGF-β-induced suppression of CTSL expression and secretion.

pLFs sequester CTSL in EVs upon TGF-β stimulation

Since CTSL has been shown to localize to EVs in cell lines other than lung fibroblasts [16, 17], we investigated whether CTSL is also secreted in EVs of pLFs and whether this localization is affected by TGF-β. We quantified EV size and concentration using nanoparticle tracking analysis (NTA) (Fig. 4A). pLFs activated with TGF-β packaged more CTSL into secreted EVs compared with vehicle-treated pLFs (4.5-fold ± 0.7673; $P < 0.05$) (Fig. 4B). The form detected in EVs was the less active pro-form of CTSL (42 kDa). We therefore assessed whether CTSL in EVs retains activity as measured by NC1 domain cleavage. To do so, we localized our NC1-Flag recombinant protein to EVs by overexpressing it in MRC-5 cells (supplementary Fig. S4, available at *Rheumatology* online). We then treated NC1-Flag-expressing MRC-5 fibroblasts with TGF-β or vehicle. NC1-Flag in EVs showed no cleavage in both treatment groups with no evidence of mature CTSL (Fig. 4C). The data suggest that TGF-β sequesters the less active pro-form of CTSL into EVs released from pLFs, further contributing to reduced availability of CTSL in the ECM.

SSc-derived pLFs express lower levels of CTSL and sequester more CTSL in EVs than normal pLFs

Since lung fibroblasts are the effector cells in SSc-related lung fibrosis [21], we investigated whether SSc-derived pLFs express lower baseline levels of CTSL than NL pLFs. Using RNA sequencing, we found that *CTSL* expression is significantly reduced in SSc pLFs compared with NL pLFs (log2FC = −1.1402; q-value = 7.09×10^{-4}). Clustering analysis showed that *CTSL* clustered similarly to known antifibrotic genes that were differentially downregulated in SSc pLFs, unlike profibrotic genes whose expressions were increased in SSc pLFs (Fig. 5A). We confirmed the RNA-seq data by comparing baseline gene expression in NL and SSc pLFs. Our results show that SSc pLFs express significantly less *CTSL* than their NL counterparts at both the mRNA level (0.72-fold ± 0.071; $P < 0.05$) (Fig. 5B) and the protein level (Fig. 5C) (0.52-fold ± 0.066; $P < 0.05$). When comparing expression of *COL18A1*, we found that SSc pLFs show significantly higher expression than NL pLFs at baseline (3.238-fold ± 0.6997; $P < 0.05$). The decrease in *CTSL* and increase in *COL18A1* expression in SSc *vs*

FIG. 4 TGF-β increases packaging CTSL into EV, where it remains inactive

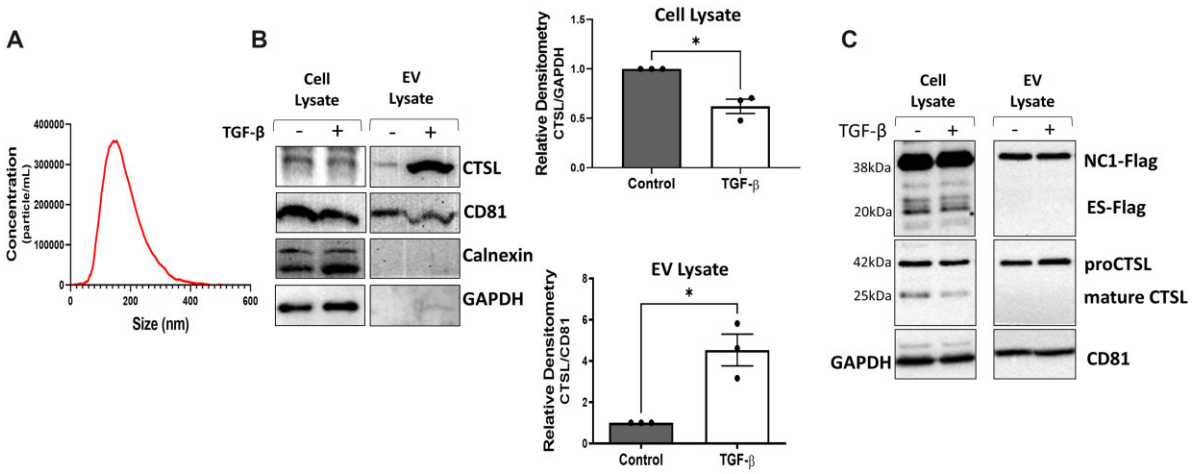

NL fibroblasts from different donors were treated with vehicle control or recombinant TGF-β. Supernatants and lysates were collected after 48 h of stimulation. EV were isolated from supernatants and lysed. (**A**) EV size and concentration were quantified using NTA. (**B**) EV content of CTSL, CD81 and Calnexin (negative control) were analysed by immunoblotting upon loading equal EV number in each lane. Cellular lysates were analysed as well for proof of successful EV isolation ($n = 3$, thee donors). Densitometry analysis was performed. The CTSL/CD81 ratio in the EV fractions was calculated as an indicator of the extent of CTSL packaging in EV. Graphs (right panels) analysed by paired sample *t*-test. Bars represent mean (S.E.M.). (**C**) NC1-Flag was localized to the EVs of MRC-5 cells via overexpression, then cells were treated with vehicle control or recombinant TGF-β. EVs and lysates were collected after 48 h of stimulation. NC1-Flag, cleavage product ES-Flag and CTSL (pro and mature) were detected via immunoblotting in cellular and EV lysates ($n = 3$). GAPDH was used as a loading control for cellular lysates, and CD81 (EV marker) was used as a reference for EV lysates. EV: extracellular vesicles; ES: endostatin; CTSL: Cathepsin L; NL: normal lung; NTA: nanoparticle tracking analysis; GAPDH: glyceraldehyde-3-phosphate dehydrogenase.

NL pLFs were in concordance with the results from TGF-β-treated NL pLFs (Fig. 1B–D). Similarly, SSc pLFs sequester more CTSL into EVs than NL pLFs (3.11-fold ± 0.484; $P < 0.05$) (Fig. 5E). To investigate the role of the TGF-β Smad pathway on CTSL expression and localization in SSc, we treated SSc pLFs with SIS3, which restored *CTSL* gene expression (2.145-fold ± 0.289; $P < 0.05$), while expectedly suppressing *COL1A1* expression (0.223-fold ± 0.065; $P < 0.001$) (Fig. 5F and G). At the protein level, SIS3 induced CTSL expression and its secretion into the media (2.589-fold ± 0.27; $P < 0.05$), yet no significant change in EV levels of CTSL was observed (1.165-fold ± 0.284; $P > 0.05$) (Fig. 5H). These data demonstrate that CTSL is an antifibrotic protein whose expression and secretion freely into the ECM are suppressed in SSc pLFs via the TGF-β/Smad pathway.

SSc-derived lung tissues express lower levels of CTSL than normal lung tissues

To extend our findings to human lung tissues, we then investigated the effect of TGF-β on CTSL levels *ex vivo* in human lung tissue cores maintained in organ culture. Gene expression levels of *CTSL* were significantly reduced (0.693-fold ± 0.038; $P < 0.01$) in NL lung tissues after 72 h of TGF-β treatment (Fig. 6A). This was mirrored at the protein level with a significant reduction in CTSL protein levels at 96 h post TGF-β treatment (0.375-fold ± 0.088; $P < 0.001$), as analysed via immunofluorescence of sections of lung tissue cores (supplementary Fig. S5A and B, available at *Rheumatology* online). Finally, to extend our findings to SSc lung tissues, we assessed CTSL levels via immunofluorescence in sections of lung tissues derived from five SSc *vs* five NL donors (Fig. 6B). CTSL levels were significantly lower in SSc compared with NL lung tissue sections (0.515-fold ± 0.0997; $P < 0.01$) (supplementary Fig. S6A, available at *Rheumatology* online). As expected, the amount of tissue per field, as indicated by nuclear count via DAPI stain, was significantly higher in SSc tissues compared with NL tissues (1.786 ± 0.153; $P < 0.001$) due to the fibrotic phenotype of the latter (supplementary Fig. S6B, available at *Rheumatology* online). Thus, we normalized CTSL expression to DAPI count to compare expression relative to cell number, which resulted in even more significant reduction in CTSL levels in SSc compared with NL lungs (0.305-fold ± 0.058, $P < 0.0001$) (Fig. 6C). To investigate the type of cells expressing CTSL in NL *vs* SSc lung tissues, we co-stained for CTSL and alpha smooth muscle actin (α-SMA), a marker of myofibroblasts, as well as prosurfactant protein C (pro-SPC), a marker of alveolar epithelial type 2 cells. We noticed that SSc lung tissues with increased α-SMA expression showed minimal to no expression of CTSL compared with NL (Fig. 6D and supplementary Fig. S7A, available at *Rheumatology* online), while areas with CTSL expression in both NL and SSc

FIG. 5 SSc-derived pLFs express lower levels of CTSL and sequester more CTSL in EVs than normal pLFs

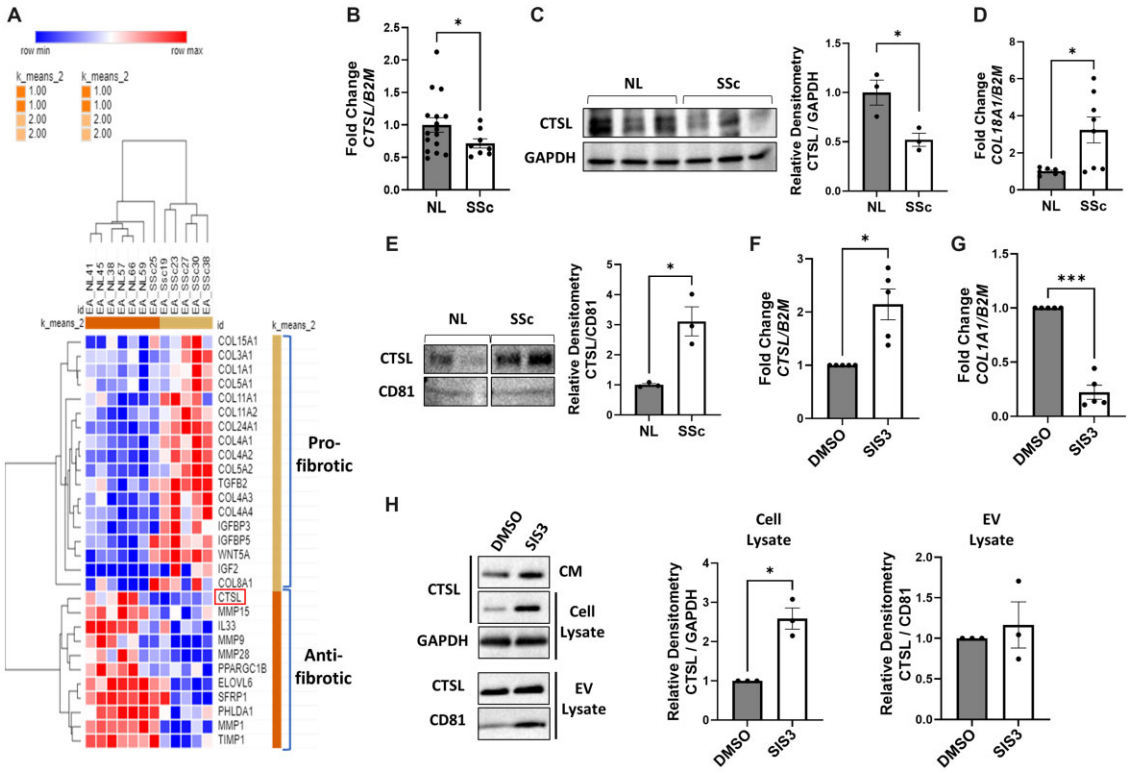

(**A**) RNA-seq data comparing RNA expression of pro and antifibrotic genes between five independent SSc-derived pLFs *vs* five independent NL-derived pLFs. *CTSL* indicated in red box. (**B**) Fold change in baseline *CTSL* gene expression levels were quantified using qPCR comparing NL ($n = 16$) *vs* SSc ($n = 8$) derived pLFs (normalized to *B2M*). (**C**) CTSL protein levels in cell lysates of NL ($n = 3$) and SSc ($n = 3$) pLFs in passage 3 were analysed by immunoblotting. GAPDH was used as a loading control for densitometry analysis. (**D**) Fold change in baseline *COL18A1* gene expression levels were quantified using qPCR comparing NL ($n = 7$) *vs* SSc ($n = 8$) derived pLFs (normalized to B2M). (**E**) EV content of CTSL and CD81 in NL ($n = 3$) and SSc ($n = 3$) was analysed by immunoblotting (representative blot shown), and CTSL/CD81 densitometry ratio was measured. Gene expression levels of (**F**) *CTSL* and (**G**) *COL1A1* were quantified using qPCR ($n = 5$, 3 independent SSc donors), and fold-change estimates were calculated to compare SIS3-treated pLFs with the DMSO-treated pLFs (normalized to *B2M*). (**H**) CTSL protein levels were analysed by immunoblotting in CM, cell lysates and EV lysates. GAPDH was used as a loading control for cell lysates, and CD81 as a reference for EV lysates, to which relative densitometry analysis was performed ($n = 3$, two independent SSc donors). Graphical presentation of the data analysed by paired sample *t*-test for SIS3- *vs* DMSO-treated pLFs, and unpaired sample *t*-test for NL *vs* SSc pLFs. Bars represent mean (S.E.M.). $^{*}P < 0.05$, $^{***}P < 0.001$. pLF: primary human lung fibroblast; CTSL: Cathepsin L; EV: extracellular vesicles; COL18A1: Collagen type XVIII alpha 1 chain; B2M: β2-microglobulin; CM: conditioned media; NL: normal lung; GAPDH: glyceraldehyde-3-phosphate dehydrogenase.

co-localized with pro-SPC (Fig. 6E and supplementary Fig. S7B, available at *Rheumatology* online). Thus, our data demonstrate that SSc lungs express reduced levels of CTSL when compared with NL lungs, which is driven by activated myofibroblasts.

Discussion

We previously reported that ES is a potent antifibrotic peptide [7, 8]. CTSL is the most efficient proteinase known to cleave and release ES from Collagen-XVIII [12, 13]. While ES is detected in the circulation and bronchoalveolar lavage fluid of SSc patients [10, 11], it does not reach anti-fibrotic levels [8], suggesting that reduced ES release via decreased CTSL expression is a potential mechanism which promotes lung fibrosis in SSc.

TGF-β signalling plays a central role in fibrosis initiation and progression, in part via its effect on fibroblast activation [20, 21]. This is especially true in SSc-related fibrosis, where fibrotic genes downstream of TGF-β were shown to be upregulated in fibrotic lungs and skin of SSc patients [22, 23, 28, 29]. We therefore investigated the effect of TGF-β on Collagen-XVIII and ES levels in pLFs, the effector cells in fibrosis [21]. We showed that while ES generation is significantly reduced, Collagen XVIII expression is increased by TGF-β. This suggests that the TGF-β-induced reduction in ES levels cannot be

FIG. 6 SSc-derived lung tissues have lower levels of CTSL than normal lung tissues

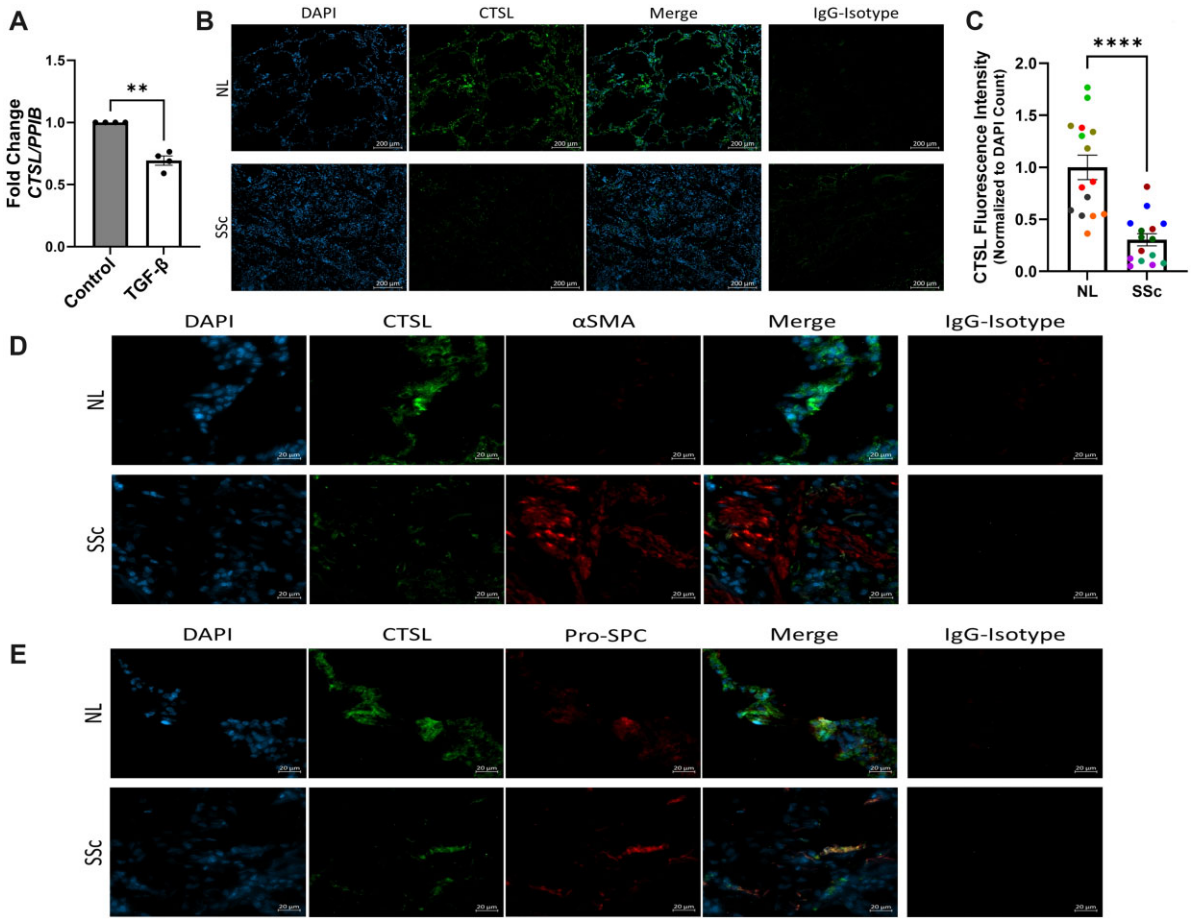

(**A**) *CTSL* gene expression levels in TGF-β-treated NL tissues were quantified using qPCR, and fold-change estimates were calculated to compare TGF-β to vehicle (normalized to *PPIB*). ($n = 4$, four donors). (**B**) Representative images of immunofluorescence staining of NL *vs* SSc sections showing CTSL expression (green) and nuclear DAPI staining (blue) (scale = 200 μm). (**C**) Normalization of CTSL intensity to DAPI count as a representation of CTSL expression relative to tissue amount per field (fold change). Each colour represents a donor. Three fields were used from each of $n = 5$ independent NL donors and $n = 5$ independent SSc donors. (**D**) Representative images of co-immunofluorescence staining of NL and SSc sections showing CTSL expression (green), α-SMA (red) or (**E**) pro-SPC (red) and nuclear DAPI staining (blue) (Scale = 20 μm). Bars in panels (A) and (C) represent mean (S.E.M.). $^{**}P < 0.01$, $^{****}P < 0.0001$. CTSL: Cathepsin L; COL18A1: Collagen type XVIII alpha 1 chain; PPIB: Peptidylprolyl Isomerase B; NL: normal lung.

explained by the downregulation of its parent protein, Collagen XVIII, but rather by a post-translational cleavage event. In fact, the increase in Collagen XVIII expression could be serving as a potential compensatory mechanism for the insufficient ES levels by increasing expression of the parent protein. Recently, Ojalill *et al.* showed that while human prostate fibroblasts can accumulate Collagen XVIII in the ECM, endostatin was only cleaved from the NC1 domain when CTSL was available [30]. This further supports the original study by Felbor *et al.* showing that murine CTSL generates endostatin from Collagen XVIII [12], which was later demonstrated for human CTSL as well [13]. With the evidence highlighting the role of CTSL in ES generation from Collagen XVIII, we sought to study the effect of TGF-β-driven lung fibrosis on CTSL expression, secretion and activity responsible for the release of ES.

Our data indicated that following TGF-β activation, pLFs reduced the availability of CTSL in the ECM, where it could otherwise activate ES. This occurred in both a direct and an indirect manner. Directly, TGF-β inhibited CTSL expression at the transcriptional level, followed by a consequent reduction in CTSL protein secretion. The secretion of CTSL is needed to generate ES from Collagen XVIII [12]. Since ES is a potent antifibrotic protein [7, 8], it is possible that its blunted release, via reduced availability of CTSL in the extracellular milieu, is a mechanism by which lung fibrosis is promoted in SSc

patients. Interestingly, recent studies have shown that CTSL gene and protein expression are inversely associated with fibrosis progression. In mice, Zhang *et al.* showed reduced CTSL protein expression in kidneys post-unilateral ureter obstruction (UUO)-induced fibrosis [15]. In the same study, CTSL knockout mice had significantly increased collagen deposition and worsened kidney fibrosis post-UUO compared with wildtype mice [15]. Furthermore, Yamashita *et al.* demonstrated that serum CTSL protein levels in SSc patients were inversely correlated with severity of dermal fibrosis [14]. They also showed reduced *CTSL* mRNA expression in bleomycin-induced fibrotic skin of mice [14].

Mechanistically, we show that the CTSL transcriptional suppression is governed by the TGF-β canonical pathway (Smad-dependent pathway) as the reduction in CTSL levels was abrogated with a selective Smad3 inhibitor [27]. Interestingly, the inhibitor alone significantly induced CTSL expression, which suggests that the canonical pathway suppresses CTSL expression in a constitutive fashion. In fact, the Smad pathway has been shown to constitutively play a homeostatic role in fibroblasts, as Huang *et al.* demonstrated the importance of fibroblast-specific Smad3 in regulating baseline collagen synthesis [31]. Smad3 activation and translocation of the Smad2/3/4 complex to the nucleus can result in *CTSL* gene regulation since the CTSL promoter contains Smad-binding elements [32]. This binding can result in activation or repression of gene expression. For example, repression of gene expression by TGFβ-activated Smad3 was shown by Ali *et al.* who demonstrated that TGF-β represses expression of REGγ in a TGF-β Smad-dependent manner in H1299 and HaCat cells [33]. Since upregulated TGF-β signalling has been demonstrated in SSc tissues [22, 34], it is plausible that a constitutively suppressed CTSL production is a contributing factor to the development of lung fibrosis. In contrast, blocking major noncanonical pathways with different specific inhibitors did not abrogate the TGF-β-induced reduction of CTSL, but rather further reduced it. This might be due to the amplification of the canonical pathway upon blocking other TGF-β downstream pathways [20], further implicating the Smad-dependent pathway in inhibiting CTSL expression.

TGF-β also indirectly reduced CTSL availability by sequestering available pro-CTSL into secreted EVs, limiting its otherwise activation and access to Collagen XVIII. Using isotope pulse/trace proteomics in hypothalamic cells, *Tan et al.* showed evidence that newly synthesized and pre-existing pro-CTSL can exhibit preferential localization into EVs [17]. Moreover, many studies have shown that inhibition of lysosomal function, such as in lysosomal storage diseases and neurodegenerative diseases, increases release of EVs [35, 36]. This phenomenon is thought to maintain homeostasis by compensating for the impaired protein degradation intracellularly [35]. Since TGF-β reduces expression and secretion of pro-CTSL by pLFs, it is possible that the intracellular accumulation of a pool of CTSL triggers its release into EVs. It is important to note that autoactivation of pro-CTSL into mature active CTSL is dependent on the low pH environment of the lysosomal lumen, after which CTSL is secreted freely into the extracellular space via lysosomal exocytosis [16, 37]. Even pro-CTSL secreted into the extracellular space can encounter an acidic microenvironment that allows for activation and prolonged activity of mature CTSL [16, 38]. While we and others show that only the pro-form of CTSL is found in EVs [17], our data further suggest that pro-CTSL is not activated in pLF-derived EVs, since there was no cleavage of EV-localized NC1-Flag. Further studies are needed to assess whether recipient cells could potentially activate the pro-CTSL delivered via EVs.

Translating our findings using SSc pLFs and lung tissues confirmed that *CTSL* expression is significantly downregulated in SSc when compared with normal donor pLFs and lung tissues, and the decreased CTSL levels are attributed to myofibroblasts. Our previous microarray analysis of SSc lung tissues and fibroblasts confirms decreased CTSL levels in SSc as well as in idiopathic pulmonary fibrosis [23], suggesting that reduced CTSL levels is a shared feature of pulmonary fibrosis across the two diseases. In fact, clustering analysis of known profibrotic and antifibrotic genes in our RNA sequencing data clustered *CTSL* with the antifibrotic group of genes that were similarly downregulated in SSc pLFs, such as *IL33*, *SFRP1*, *PPARG*, *ELOVL6*, *PHLDA1* and others [39–43]. This supports the antifibrotic role of CTSL in healthy lungs. In addition, multiple studies have shown TGF-β to be central in SSc-related lung fibrosis [22]. Christmann *et al.* demonstrated that lung tissues from biopsied SSc patients showed increased expression of TGF-β-regulated genes which correlated with progressive lung fibrosis [44]. Further, we previously reported that SSc-derived pLFs expressed higher *TGFB1* mRNA levels at baseline than healthy pLFs [45]. Thus, there is increasing evidence demonstrating that TGF-β expression is constitutively augmented in SSc pathology. In fact, downstream canonical Smad3 phosphorylation and its nuclear localization were found to be constitutively elevated in SSc-derived fibroblasts [46]. In that sense, constitutive TGF-β/Smad-driven suppression of CTSL expression and secretion by pLFs in SSc lung parenchyma effectively reduces release of ES and its antifibrotic effects.

Taken together, our data implicate the TGF-β–CTSL–ES axis as a novel pathway in SSc-associated lung fibrosis. Since TGF-β is a pleiotropic signalling molecule with important physiological roles, targeting it as a fibrotic therapy for SSc has led to serious adverse events [47, 48]. Therefore, current efforts are focused on targeting molecules downstream of TGF-β. Although various mechanisms have been identified in lung fibrosis, our study highlights CTSL as an important protein for the anti-fibrotic response and suggests that inducing its endogenous expression in fibrotic lung diseases in SSc and idiopathic pulmonary fibrosis is a viable therapeutic

strategy to reduce lung fibrosis, by boosting release of its anti-fibrotic target, ES.

Acknowledgements

J.E.M. and C.F.-B. designed the experiments, J.E.M. performed the research, and collected and analysed data, S.S. contributed to experimental design, L.R. analysed data, J.P.M. and S.N.N. acquired human tissues, J.E.M. wrote the first draft, J.E.M., S.S., L.R. and C.F.-B. interpreted data and contributed to manuscript writing; all authors edited and approved the final version.

Funding: This work was supported by the National Scleroderma Foundation via a pre-doctoral award (J.E.M.), K24 AR060297 (C.F.-B.), T32 AR050958 (L.R.) and T32 HL144470 (S.S.).

Disclosure statement: The authors have declared no conflicts of interest.

Data availability statement

The data are included in the article and the accompanying supplementary material.

Supplementary data

Supplementary data are available at *Rheumatology* online.

References

1 Wynn TA, Ramalingam TR. Mechanisms of fibrosis: therapeutic translation for fibrotic disease. Nat Med 2012; 18:1028–40.

2 Ho YY, Lagares D, Tager AM, Kapoor M. Fibrosis–a lethal component of systemic sclerosis. Nat Rev Rheumatol 2014;10:390–402.

3 Elhai M, Meune C, Boubaya M *et al.*; EUSTAR group. Mapping and predicting mortality from systemic sclerosis. Ann Rheum Dis 2017;76:1897–905.

4 Khanna D, Lin CJF, Furst DE *et al.*; focuSSced investigators. Tocilizumab in systemic sclerosis: a randomised, double-blind, placebo-controlled, phase 3 trial. Lancet Respir Med 2020;8:963–74.

5 Distler O, Highland KB, Gahlemann M *et al.*; SENSCIS Trial Investigators. Nintedanib for systemic sclerosis-associated interstitial lung disease. N Engl J Med 2019; 380:2518–28.

6 Zatterstrom UK, Felbor U, Fukai N, Olsen BR. Collagen XVIII/endostatin structure and functional role in angiogenesis. Cell Struct Funct 2000;25:97–101.

7 Nishimoto T, Mlakar L, Takihara T, Feghali-Bostwick C. An endostatin-derived peptide orally exerts anti-fibrotic activity in a murine pulmonary fibrosis model. Int Immunopharmacol 2015;28:1102–5.

8 Yamaguchi Y, Takihara T, Chambers RA *et al.* A peptide derived from endostatin ameliorates organ fibrosis. Sci Transl Med 2012;4:136ra71.

9 Sharma S, Watanabe T, Nishimoto T *et al.* E4 engages uPAR and enolase-1 and activates urokinase to exert antifibrotic effects. JCI Insight 2021;6:e144935.

10 Hebbar M, Peyrat JP, Hornez L *et al.* Increased concentrations of the circulating angiogenesis inhibitor endostatin in patients with systemic sclerosis. Arthritis Rheum 2000;43:889–93.

11 Richter AG, McKeown S, Rathinam S *et al.* Soluble endostatin is a novel inhibitor of epithelial repair in idiopathic pulmonary fibrosis. Thorax 2009;64:156–61.

12 Felbor U, Dreier L, Bryant RA *et al.* Secreted cathepsin L generates endostatin from collagen XVIII. EMBO J 2000; 19:1187–94.

13 Ferreras M, Felbor U, Lenhard T, Olsen BR, Delaissé J. Generation and degradation of human endostatin proteins by various proteinases. FEBS Lett 2000;486:247–51.

14 Yamashita T, Asano Y, Taniguchi T *et al.* A potential contribution of altered cathepsin L expression to the development of dermal fibrosis and vasculopathy in systemic sclerosis. Exp Dermatol 2016;25:287–92.

15 Zhang X, Zhou Y, Yu X *et al.* Differential roles of cysteinyl cathepsins in TGF-β signaling and tissue fibrosis. iScience 2019;19:607–22.

16 Yadati T, Houben T, Bitorina A, Shiri-Sverdlov R. The ins and outs of cathepsins: physiological function and role in disease management. Cells 2020;9:1679.

17 Tan CF, Teo HS, Park JE *et al.* Exploring extracellular vesicles biogenesis in hypothalamic cells through a heavy isotope pulse/trace proteomic approach. Cells 2020;9:1320.

18 Van Niel G, D'Angelo G, Raposo G. Shedding light on the cell biology of extracellular vesicles. Nat Rev Mol Cell Biol 2018;19:213–28.

19 McVey MJ, Maishan M, Blokland KEC, Bartlett N, Kuebler WM. Extracellular vesicles in lung health, disease, and therapy. Am J Physiol Lung Cell Mol Physiol 2019;316:L977–89.

20 Frangogiannis NG. Transforming growth factor–β in tissue fibrosis. J Exp Med 2020;217:e20190103.

21 Garrett SM, Baker Frost D, Feghali-Bostwick C. The mighty fibroblast and its utility in scleroderma research. J Scleroderma Relat Disord 2017;2:69–134.

22 Lafyatis R. Transforming growth factor β–at the centre of systemic sclerosis. Nat Rev Rheumatol 2014;10:706–19.

23 Hsu E, Shi H, Jordan RM *et al.* Lung tissues in patients with systemic sclerosis have gene expression patterns unique to pulmonary fibrosis and pulmonary hypertension. Arthritis Rheum 2011;63:783–94.

24 Pilewski JM, Liu L, Henry AC, Knauer AV, Feghali-Bostwick CA. Insulin-like growth factor binding proteins 3 and 5 are overexpressed in idiopathic pulmonary fibrosis and contribute to extracellular matrix deposition. Am J Pathol 2005;166:399–407.

25 Nguyen XX, Nishimoto T, Takihara T *et al.* Lysyl oxidase directly contributes to extracellular matrix production and

fibrosis in systemic sclerosis. Am J Physiol Lung Cell Mol Physiol 2021;320:L29–40.

26 Takamura N, Renaud L, da Silveira WA, Feghali-Bostwick C. PDGF promotes dermal fibroblast activation via a novel mechanism mediated by signaling through MCHR1. Front Immunol 2021;12:745308.

27 Jinnin M, Ihn H, Tamaki K. Characterization of SIS3, a novel specific inhibitor of Smad3, and its effect on transforming growth factor-β1-induced extracellular matrix expression. Mol Pharmacol 2006;69:597–607.

28 Malaab M, Renaud L, Takamura N *et al.* Antifibrotic factor KLF4 is repressed by the miR-10/TFAP2A/TBX5 axis in dermal fibroblasts: insights from twins discordant for systemic sclerosis. Ann Rheum Dis 2022; 81:268–77.

29 Renaud L, da Silveira WA, Takamura N, Hardiman G, Feghali-Bostwick C. Prominence of IL6, IGF, TLR, and bioenergetics pathway perturbation in lung tissues of scleroderma patients with pulmonary fibrosis. Front Immunol 2020;11:383.

30 Ojalill M, Virtanen N, Rappu P *et al.* Interaction between prostate cancer cells and prostate fibroblasts promotes accumulation and proteolytic processing of basement membrane proteins. Prostate 2020;80: 715–26.

31 Huang S, Chen B, Humeres C *et al.* The role of Smad2 and Smad3 in regulating homeostatic functions of fibroblasts in vitro and in adult mice. Biochim Biophys Acta Mol Cell Res 2020;1867:118703.

32 Zhao Y, Shen X, Zhu Y *et al.* Cathepsin L-mediated resistance of paclitaxel and cisplatin is mediated by distinct regulatory mechanisms. J Exp Clin Cancer Res 2019;38:333.

33 Ali A, Wang Z, Fu J *et al.* Differential regulation of the REGγ–proteasome pathway by p53/TGF-β signalling and mutant p53 in cancer cells. Nat Commun 2013;4:2667.

34 Wei J, Fang F, Lam AP *et al.* Wnt/β-catenin signaling is hyperactivated in systemic sclerosis and induces Smad-dependent fibrotic responses in mesenchymal cells. Arthritis Rheum 2012;64:2734–45.

35 Palmulli R, van Niel G. To be or not to be… secreted as exosomes, a balance finely tuned by the mechanisms of biogenesis. Essays Biochem 2018;62:177–91.

36 Villarroya-Beltri C, Baixauli F, Mittelbrunn M *et al.* ISGylation controls exosome secretion by promoting lysosomal degradation of MVB proteins. Nat Commun 2016;7:13588.

37 Castro-Gomes T, Corrotte M, Tam C, Andrews NW. Plasma membrane repair is regulated extracellularly by proteases released from lysosomes. PLoS ONE 2016;11: e0152583.

38 Uhlman A, Folkers K, Liston J, Pancholi H, Hinton A. Effects of vacuolar H+-ATPase inhibition on activation of Cathepsin B and Cathepsin L secreted from MDA-MB231 breast cancer cells. Cancer Microenviron 2017; 10:49–56.

39 Gatti F, Mia S, Hammarström C *et al.* Nuclear IL-33 restrains the early conversion of fibroblasts to an extracellular matrix-secreting phenotype. Sci Rep 2021;11: 108.

40 De Langhe E, Aznar-Lopez C, De Vooght V *et al.* Secreted frizzled related proteins inhibit fibrosis in vitro but appear redundant in vivo. Fibrogenesis Tissue Repair 2014;7:14.

41 Lakatos HF, Thatcher TH, Kottmann RM *et al.* The role of PPARs in lung fibrosis. PPAR Res 2007;2007:1–10.

42 Sunaga H, Matsui H, Ueno M *et al.* Deranged fatty acid composition causes pulmonary fibrosis in Elovl6-deficient mice. Nat Commun 2013;4:2563.

43 Kwapiszewska G, Gungl A, Wilhelm J *et al.* Transcriptome profiling reveals the complexity of pirfenidone effects in idiopathic pulmonary fibrosis. Eur Respir J 2018;52:1800564.

44 Christmann RB, Sampaio-Barros P, Stifano G *et al.* Association of interferon- and transforming growth factor β-regulated genes and macrophage activation with systemic sclerosis-related progressive lung fibrosis. Arthritis Rheumatol 2014;66:714–25.

45 Garrett SM, Hsu E, Thomas JM, Pilewski JM, Feghali-Bostwick C. Insulin-like growth factor (IGF)-II- mediated fibrosis in pathogenic lung conditions. PLoS ONE 2019; 14:e0225422.

46 Mori Y, Chen S-J, Varga J. Expression and regulation of intracellular SMAD signaling in scleroderma skin fibroblasts. Arthritis Rheum 2003;48:1964–78.

47 Györfi AH, Matei AE, Distler JHW. Targeting TGF-β signaling for the treatment of fibrosis. Matrix Biol 2018; 68–69:8–27.

48 Denton CP, Merkel PA, Furst DE *et al.*; Cat-192 Study Group, Scleroderma Clinical Trials Consortium. Recombinant human anti–transforming growth factor β1 antibody therapy in systemic sclerosis: a multicenter, randomized, placebo-controlled phase I/II trial of CAT-192. Arthritis Rheum 2007;56:323–33.